Environmental Science & Technology Letters

pubs.acs.org/journal/estlcu

Letter

Efficient Photocatalytic PFOA Degradation over Boron Nitride

Lijie Duan,[○] Bo Wang,[○] Kimberly Heck, Sujin Guo, Chelsea A. Clark, Jacob Arredondo, Minghao Wang, Thomas P. Senftle, Paul Westerhoff, Xianghua Wen, Yonghui Song,* and Michael S. Wong*

Cite This: https://dx.doi.org/10.1021/acs.estlett.0c00434

Read Online

ACCESS | Metrics & More | Article Recommendations | Supporting Information

ABSTRACT: Concern over water contamination by per/polyfluoroalkyl substances (PFAS) has highlighted the lack of effective treatment approaches. Photocatalysis offers advantages of using ambient conditions for reaction, air as the oxidant, and light as the energy source, but identifying photoactive materials is challenging. Herein, we report that boron nitride (BN) degrades PFOA upon irradiation with 254 nm light. The ability of BN to degrade PFOA photocatalytically has previously been unreported and is unexpected, because its band gap is too large for light absorption. On the basis of scavenger results, we suggest that PFOA degrades in the presence of BN via a hole-initiated reaction pathway similar to the TiO_2 case and involves superoxide/hydroperoxyl and hydroxyl radicals. We surmised that defects allow BN to absorb in the UVC range and to photogenerate reactive oxygen species. Sealed batch studies indicated BN was ~2 and ~4 times more active than TiO_2, before and after ball milling the material, respectively. BN can be reused, showing no decrease in activity over three cycles. BN was active for the photocatalytic degradation of GenX, another PFAS of concern. These findings present fresh opportunities for materials design and for the re-evaluation of other wide band gap semiconductors for PFAS photocatalytic degradation.

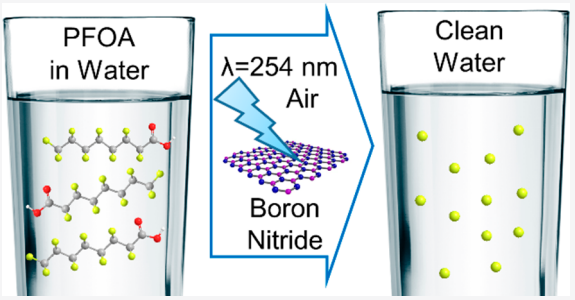

1. INTRODUCTION

Perfluorocarboxylic acids ($C_nF_{2n+1}COOH$, PFCAs), part of the per/polyfluoroalkyl substance (PFAS) family, have been detected in water and soil due to their application as surfactants, additives, firefighting foams, and lubricants.[1−3] Stable by design (~485 kJ/mol C−F bond),[4] the degradation of PFCAs by natural decomposition and microbiological treatment is extremely slow, with half-lives of ~50 years in water[5] and 112−233 years in soil,[6] and they are classified as persistent organic pollutants. Toxicological studies indicated that PFCAs, including perfluorooctanoic acid ($C_7F_{15}COOH$, PFOA), bioaccumulate in humans and wildlife and lead to developmental and reproductive problems, liver damage, and cancer.[7] Efficient and economical PFOA degradation technologies are urgently needed.

Numerous PFOA degradation methods are under development, including advanced oxidation processes (AOPs)[8−10] and advanced reduction processes.[11−13] UV-based AOPs promote direct and indirect photochemical reactions that show promise for efficient degradation. Vacuum ultraviolet (VUV) and UVC irradiation with high spectral irradiance (>600 mW/cm^2) were reported to decompose PFOA via photolysis.[9,14] However, defluorination is slow, making direct photolysis of PFOA unfeasible. VUV and UVC irradiation in solutions containing sulfite or persulfate also degrades PFAS,[15,16] but continuous chemical addition is required.

Heterogeneous photocatalysis can be operated in recirculating slurries that do not require continuous addition of reagent.[17] As a commercially available form of TiO_2 and a widely used photocatalyst, P25-TiO_2 is active for PFOA photodegradation though at relatively slow rates (Table S1).[18−20] Semiconductor materials with wider band gaps (i.e., in the UVC range) have been investigated for PFOA degradation. Zhao et al. synthesized β-Ga_2O_3, which exhibited a level of PFOA degradation that was higher than that of TiO_2.[21] They ascribed the activity to the reductive capability of the photogenerated electrons in the conduction band of β-Ga_2O_3. Li et al. reported photocatalytic decomposition of PFOA using In_2O_3, which showed significant activity for PFOA decomposition with a rate constant that was 8.4 times higher than that of TiO_2.[22] Sahu et al. synthesized and tested a $Bi_3O(OH)(PO_4)_2$ photocatalyst, which was more active than TiO_2.[23]

PFOA degradation occurs through different reaction mechanisms, depending on the photocatalyst composition

Received: May 27, 2020
Revised: June 4, 2020
Accepted: June 4, 2020

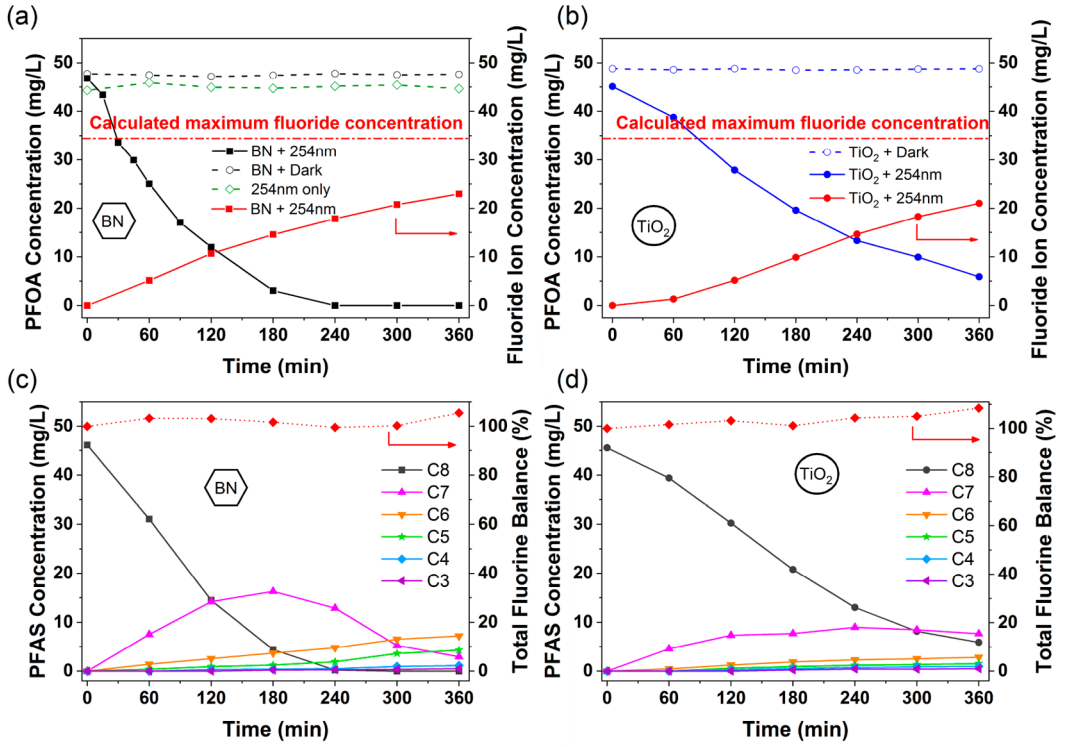

Figure 1. (a) HPLC−DAD-detected PFOA concentration−time profiles using BN and TiO_2, with and without 254 nm irradiation. (b) Fluoride concentration profiles for BN and TiO_2 with 254 nm irradiation. (c and d) HPLC−MS-detected concentration−time profiles of PFOA and byproducts for BN and TiO_2, respectively, with corresponding total fluorine balance. Reaction conditions: $[PFOA]_0 \sim 50$ ppm, dosage of 2.5 g of BN/L or 0.5 g of TiO_2/L, ambient temperature, air headspace, 254 nm light, and an initial pH of 6.5.

and reaction conditions. Many TiO_2-based studies implicate photogenerated holes as the primary oxidant species, in addition to hydroxyl radicals.[19,20,24] Studies using Fe(III) and concentrated H_2O_2 showed that superoxide/hydroperoxyl radicals are responsible for defluorination.[25] Studies using SiC photocatalysts suggest that a reductive hydrodefluorination pathway may also be possible.[4] More effective PFOA degradation may be possible through new reaction pathways.

Boron nitride (BN) is normally considered an electrical insulator due to the wideness of its band gap (~6.0 eV), but increasingly, it is being treated as a wide band gap semiconductor. Composite BN materials are now being studied for photocatalytic water splitting[26,27] and for photocatalytic water treatment.[28,29] For the latter, the BN component is proposed to increase organic contaminant adsorption[28] and to improve photocatalytic efficiency.[29] There is no evidence that BN alone has any photodegradation properties.

In this study, we report the surprising finding that commercially available BN is not only active for the heterogeneous photodegradation of PFOA at room temperature using 254 nm light but also as much as 4 times more effective than P25-TiO_2 under optimal conditions. Using radical scavengers, we find evidence for superoxide/hydroperoxyl-, hydroxyl-, and hole-promoted reaction pathways. Through diffuse-reflectance UV (DR-UV) and Raman spectroscopies, we observed the importance of defects for UVC absorption and photocatalytic activity. These results reveal the PFOA photodegradation properties of BN, expanding the spectrum of photocatalysts for targeted PFAS treatment.[30]

2. MATERIALS AND METHODS

The hexagonal phase of BN and the P25 form of TiO_2 were procured from commercial sources and used as received (Text S1). Ball milling and materials characterization are described in Text S2. XRD spectra and TEM images are shown in Figures S1 and S2, and BET surface area data are listed in Table S2. Details of the photocatalytic experiments, conducted in a custom-built reactor with six 4 W 254 nm bulbs similar to that reported by Alvarez and co-workers (Scheme S1),[31] are described in Text S3. Results of dosage experiments are shown in Figure S3, and results of additional control experiments are shown in Figures S4 and S5. Results of radical probe experiments are shown in Figure S6. Analytical methods are described in Text S4. ICP analysis of postreaction fluids showed no leaching of BN or TiO_2.

3. RESULTS AND DISCUSSION

PFOA concentrations unexpectedly decreased with irradiation time using BN (Figure 1). Irradiation was required for PFOA loss to occur; BN did not adsorb PFOA in the dark (Figure S4). PFOA did not degrade with 254 nm light without BN or TiO_2. PFOA had a half-life of 1.2 h for BN in our reaction system, exhibiting a photocatalytic rate of 0.24 mg of PFOA L^{-1} min^{-1}. PFOA degraded using TiO_2 as expected, with a half-life of 2.4 h (rate of 0.11 mg of PFOA L^{-1} min^{-1}). These studies were carried out at optimum catalyst dosages, which avoided differential reaction conditions and poor light penetration, and maximized photocatalytic rates (Figure S3).[32,33] Fluoride ions were detected after irradiation began (Figure 1b). After 240 min, ~52% of the total initial fluorine (30 mg of F/L) was released as F^- for BN (compared to ~40% for TiO_2). Also, after 240 min, PFOA concentrations were not

https://dx.doi.org/10.1021/acs.estlett.0c00434
Environ. Sci. Technol. Lett. XXXX, XXX, XXX−XXX

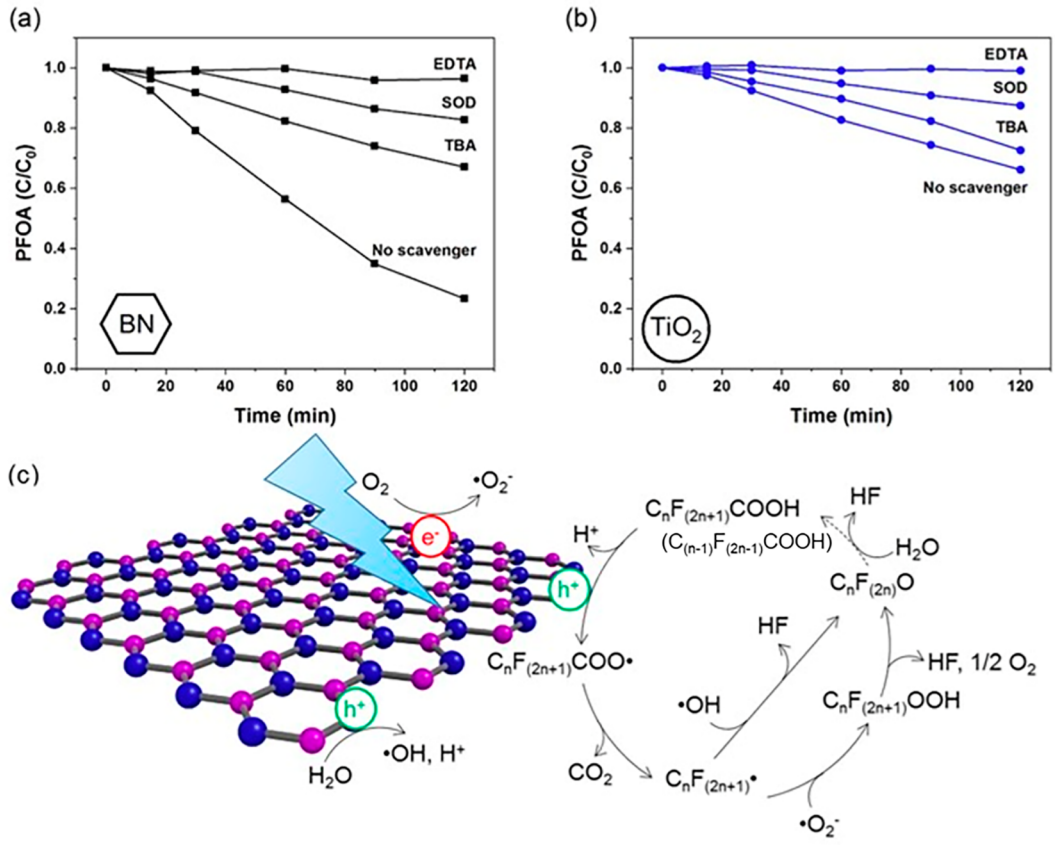

Figure 2. PFOA photodegradation over (a) BN and (b) TiO_2 using EDTA, SOD, and TBA, as hole, superoxide/hydroperoxyl, and hydroxyl radical scavengers, respectively. (c) Proposed photooxidative mechanism of PFOA degradation over BN. Reaction conditions: $[PFOA]_0 \sim 50$ ppm, 3 mM scavenger, dosage of 2.5 g of BN/L or 0.5 g of TiO_2/L, ambient temperature, air headspace, and 254 nm light.

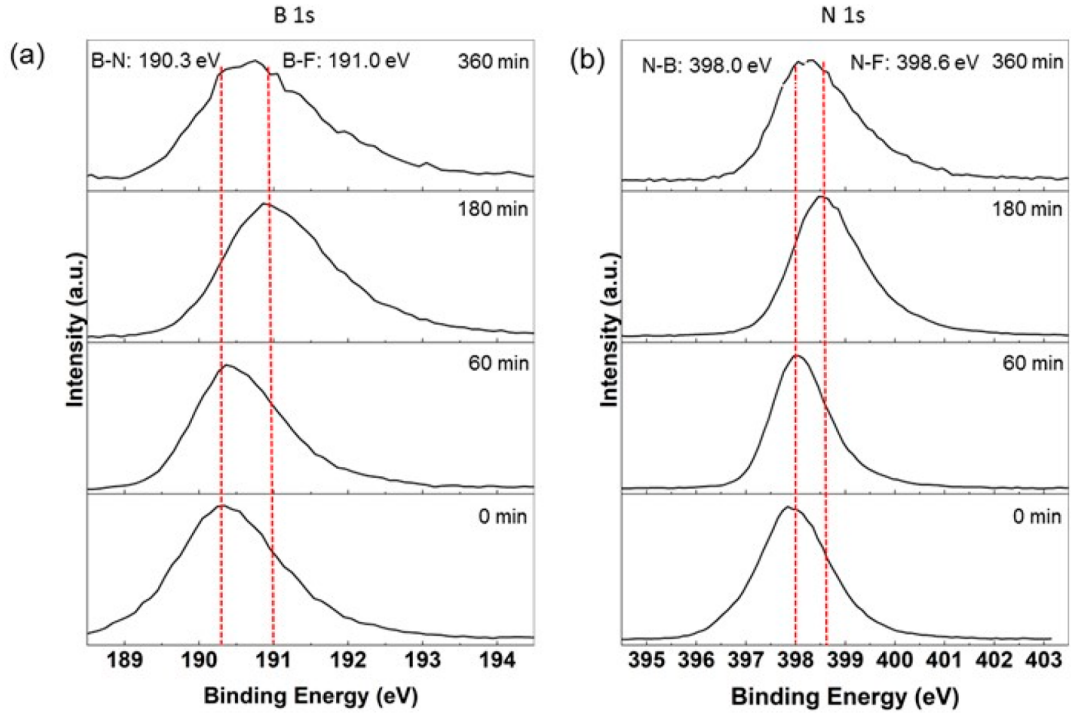

Figure 3. XPS of (a) B 1s and (b) N 1s binding energies at different reaction times. Reaction conditions: $[PFOA]_0 \sim 50$ ppm, dosage of 2.5 g of BN/L, ambient temperature, air headspace, 254 nm light, an an initial pH of 6.5.

https://dx.doi.org/10.1021/acs.estlett.0c00434
Environ. Sci. Technol. Lett. XXXX, XXX, XXX−XXX

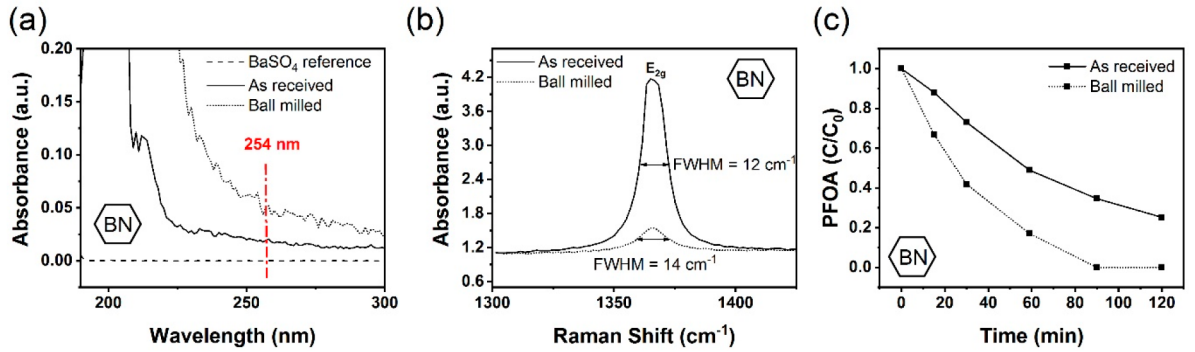

Figure 4. (a) DR-UV and (b) Raman spectra of as-received and ball-milled BN. (c) PFOA concentration−time profiles using as-received and ball-milled BN. Reaction conditions: $[PFOA]_0 \sim 50$ ppm, dosage of 2.5 g of BN/L, ambient temperature, air headspace, 254 nm light, and an initial pH of 3.3.

measurable in the BN case [HPLC−diode array detector (DAD) detection limit of 1 mg/L], suggesting the formation of shorter-chain PFAS byproducts to account for the remaining ∼16%.

Prior UV-based AOP studies indicate PFOA can undergo stepwise decarboxylation and defluorination, in which PFOA ("C8") decomposes to perfluoroheptanoic acid ("C7"), which decomposes to perfluorohexanoic acid ("C6"), etc.[9,18−20] We then measured PFOA concentrations and sought to detect reaction intermediates with chain lengths of C3−C7 though HPLC−MS (detection limit of 0.01 mg/L). Figure 1c shows concentration profiles that typify reactions occurring in series; i.e., PFOA is degrading in a stepwise decarboxylation/defluorination fashion over BN. Figure 1d shows PFOA is also degrading and forming shorter-chain intermediates over TiO_2, consistent with literature reports.[9,18,19,24] Fluoride balance was completed by accounting for the fluorine in the shorter-chain byproducts in both BN and TiO_2 cases.

To probe the involvement of different ROSs, we carried out the photocatalytic reaction in the presence of ethylenediaminetetraacetic acid (EDTA), superoxide dismutase (SOD), or *tert*-butanol (TBA) as ROS scavenging agents. EDTA completely inhibited BN and TiO_2 activity, indicating photogenerated holes are critical to PFOA degradation, in agreement with previous TiO_2 literature (Figure 2).[22] SOD initially inhibited BN and TiO_2 activity before PFOA degradation became apparent after 30 min, indicating the importance of $^{\bullet}O_2^-/^{\bullet}OOH$ species. TBA had a partial inhibitory effect, indicating that $^{\bullet}OH$ radicals are also involved in PFOA degradation. Separate experiments confirmed the existence of $^{\bullet}OH$ and $^{\bullet}O_2^-/^{\bullet}OOH$ species in both BN and TiO_2 cases (Text S3 and Figure S6).[34] Protons were generated during the reaction, such that the pH was ∼3 at the end of the reaction. In all, this suggests a co-dependent mechanism (Figure 2c) in which holes and radical species degrade PFOA and related byproducts, rather than a single radical that is responsible for defluorination.

Studies of SiC photocatalysts proposed a hydrodefluorination pathway to degrade PFOA, in which the C−F bond reacted with a hydrogenated SiC surface, such that C−H and Si−F bonds formed *in situ*.[4,35] To explore the possibility of a similar reaction with BN, we performed XPS on BN before and at different reaction times (Figure 3a,b). We attributed the higher-binding energy shifts of the B 1s and N 1s peaks (after 180 min) to the formation of surface B−F and N−F bonds, respectively.[36] We speculate that PFOA and its shorter-chain homologues can react directly with surface B−H bonds formed during irradiation. The binding energy peaks shifted back after 360 min, suggesting that surface-bound fluoride was released into solution from the BN surface, as the concentrations of PFOA and its fragments decreased. A reductive reaction pathway (C−F + B−H → C−H + B−F) over *in situ*-hydrogenated BN sites may be coexisting with the photo-oxidative pathway shown in Figure 2c. The B−H surface species would be regenerated via photocatalyzed reaction with either proton or water species, as has been reported for BN and fluorinated BN in photocatalyzed water splitting.[26,27] The XPS results imply concurrent hydrodefluorination during BN-catalyzed PFOA photodegradation, the extent of which is to be determined.

The BN band gap of ∼6 eV should be too wide for 254 nm light absorption, yet PFOA underwent apparent photocatalytic degradation over BN. We measured the absorbance spectra of BN (Figure 4a) as well as TiO_2 (Figure S7) through DR-UV. As expected, TiO_2 has a wide absorbance throughout the UV region, extending from 200 to 400 nm. In comparison, the BN spectrum showed a small peak absorbance at 208 nm, consistent with previous studies of bulk BN.[27]

BN had very small, but non-zero, absorbance at 254 nm, which we hypothesized to be due to defects within BN, i.e., edge defects or B or N vacancies (Figure 4a). We next collected Raman spectra of the BN material, focusing on the E_{2g} phonon mode at ∼1371 cm^{-1}, which arises from in-plane vibrations of N and B in opposing directions.[37] Its broadness and location are measures of defectiveness.[38] The as-received BN powder was relatively defective (Figure 4b). The full width at half-maximum (fwhm) was 12 cm^{-1}, which was broader than the value of 8 cm^{-1} for bulk powder.[38] The E_{2g} mode blue-shifted to 1367 cm^{-1}, from 1371 cm^{-1} for bulk BN.[38]

We intentionally introduced more defects through ball milling,[38] with the resulting material showing increased absorbance in the UVC range (Figure 4a) and a broader E_{2g} Raman peak (fwhm of ∼14 cm^{-1}), and a slight blue-shift to 1366 cm^{-1} was also observed (Figure 4b). Notably, the ball-milled BN showed improved performance for PFOA degradation (Figure 4c). The photocatalytic degradation rate increased from 0.24 to 0.44 mg of PFOA L^{-1} min^{-1} after ball milling; these rates were ∼2 and ∼4 times greater than that of TiO_2 [0.12 mg of PFOA L^{-1} min^{-1} (Figure S9)]. The apparent quantum yields for as-received and ball-milled BN were calculated to be 0.4% and 0.7%, respectively, higher than the value of 0.18% for TiO_2 (Text S4). We conclude that BN

https://dx.doi.org/10.1021/acs.estlett.0c00434
Environ. Sci. Technol. Lett. XXXX, XXX, XXX−XXX

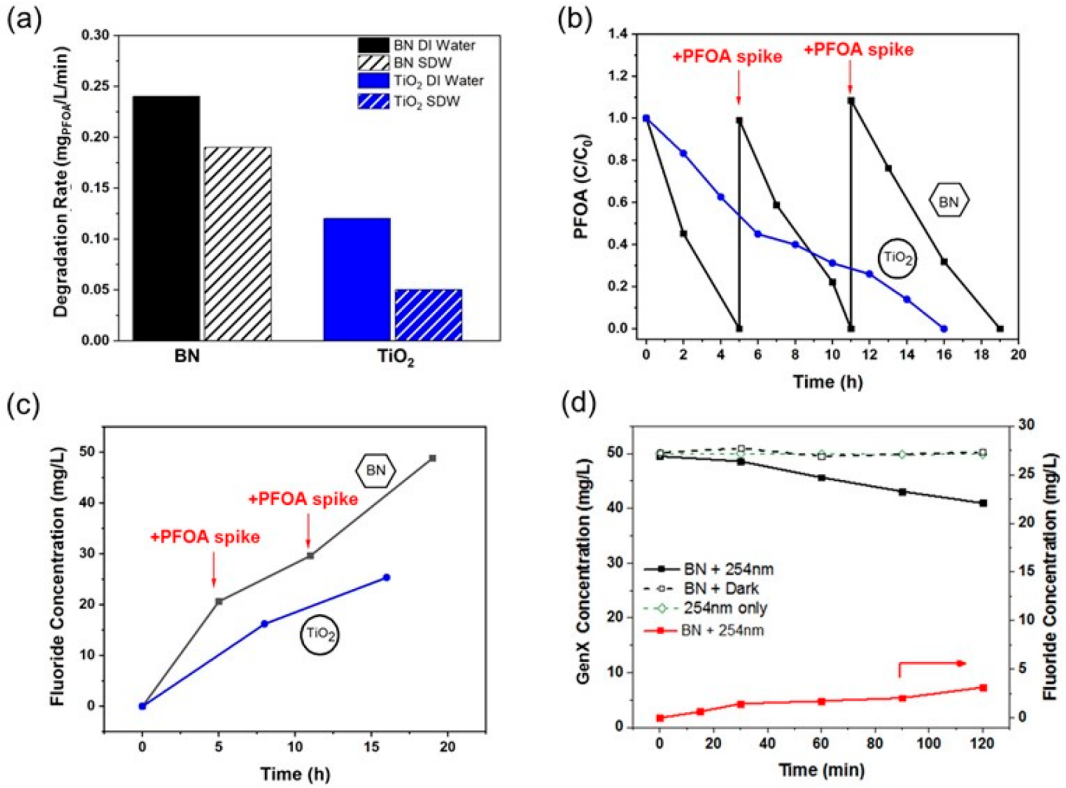

Figure 5. (a) PFOA photodegradation rates over as-received BN and TiO_2 in DI water and SDW. (b) PFOA concentration−time profiles in SDW, with reinjections of PFOA for the BN case and (c) corresponding fluoride concentration profiles. (d) GenX and fluoride concentration−time profiles using BN with 254 nm irradiation. Reaction conditions: $[PFOA]_0$ or $[GenX]_0 \sim 50$ ppm, dosage of 2.5 g of BN/L or 0.5 g of TiO_2/L, ambient temperature, air headspace, 254 nm light, and an initial pH of 3.

surface defects are necessary for light absorption and photodegradation capability and predict that large-surface area BN (for example, hydrothermally exfoliated BN), with its high surface defect content, will show higher PFOA photodegradation activity.

To determine the effects of a realistic water matrix on BN photocatalytic properties, we performed the reaction in simulated drinking water (SDW) (Table S3). Though slightly inhibited [60% vs 80% degradation in SDW vs deionized (DI) water after 120 min], BN outperformed TiO_2, whose level of degradation after 120 min dropped to 15% (Figure 5a). BN maintained activity following three cycles of PFOA degradation over 19 h, during which time the TiO_2 was able to degrade only the initial spike over 16 h (Figure 5b). At the end of the experiments, the level of free fluoride in the BN system was 48 ppm, representing ~43% of the total fluorine added, while the TiO_2 system had 25 ppm F^-, representing ~74% of the initial fluorine added (Figure 5c).

Finally, we tested BN for the photodegradation of GenX [ammonium perfluoro(2-methyl-3-oxahexanoate)], another carboxylic acid form of PFAS.[39] Roughly 20% degraded in 2 h under the same reaction conditions, with an estimated half-life of at least 5 h (Figure 5d). This is the first reported heterogeneous photocatalytic decomposition of GenX to the best of our knowledge.

■ ASSOCIATED CONTENT

Supporting Information

The Supporting Information is available free of charge at https://pubs.acs.org/doi/10.1021/acs.estlett.0c00434.

Details of materials and methods, XRD spectra, TEM images, and BET surface areas of materials, scheme of the reactor setup, catalyst dosage photocatalytic experiments, dark control experiments, terephthalic acid and nitrotetrazolium blue radical probe experiments, composition of SDW, DR-UV spectrum of TiO_2, and concentration−time profile for PFOA photodegradation over TiO_2 (PDF)

■ AUTHOR INFORMATION

Corresponding Authors

Michael S. Wong − *Department of Chemical and Biomolecular Engineering, Department of Environmental Engineering, Department of Chemistry, and Department of Materials Science and NanoEngineering, Rice University, Houston, Texas 77005, United States; Nanosystems Engineering Research Center for Nanotechnology-Enabled Water Treatment, Houston, Texas 77005, United States;* orcid.org/0000-0002-3652-3378; Email: mswong@rice.edu

Yonghui Song − *School of Environment, Tsinghua University, Beijing 100084, China; State Key Laboratory of Environmental Criteria and Risk Assessment, Chinese Research Academy of Environmental Sciences, Beijing 100012, China;* Email: songyh@craes.org.cn

Authors

Lijie Duan − *School of Environment, Tsinghua University, Beijing 100084, China; State Key Laboratory of Environmental Criteria and Risk Assessment, Chinese Research Academy of Environmental Sciences, Beijing 100012, China; Department of*

https://dx.doi.org/10.1021/acs.estlett.0c00434
Environ. Sci. Technol. Lett. XXXX, XXX, XXX−XXX

Chemical and Biomolecular Engineering, Rice University, Houston, Texas 77005, United States; Nanosystems Engineering Research Center for Nanotechnology-Enabled Water Treatment, Houston, Texas 77005, United States

Bo Wang − *Department of Chemical and Biomolecular Engineering, Rice University, Houston, Texas 77005, United States; Nanosystems Engineering Research Center for Nanotechnology-Enabled Water Treatment, Houston, Texas 77005, United States*

Kimberly Heck − *Department of Chemical and Biomolecular Engineering, Rice University, Houston, Texas 77005, United States; Nanosystems Engineering Research Center for Nanotechnology-Enabled Water Treatment, Houston, Texas 77005, United States*

Sujin Guo − *Nanosystems Engineering Research Center for Nanotechnology-Enabled Water Treatment, Houston, Texas 77005, United States; Department of Environmental Engineering, Rice University, Houston, Texas 77005, United States*

Chelsea A. Clark − *Department of Chemical and Biomolecular Engineering, Rice University, Houston, Texas 77005, United States; Nanosystems Engineering Research Center for Nanotechnology-Enabled Water Treatment, Houston, Texas 77005, United States*

Jacob Arredondo − *Department of Chemical and Biomolecular Engineering, Rice University, Houston, Texas 77005, United States*

Minghao Wang − *School of Environment, Tsinghua University, Beijing 100084, China; State Key Laboratory of Environmental Criteria and Risk Assessment, Chinese Research Academy of Environmental Sciences, Beijing 100012, China*

Thomas P. Senftle − *Department of Chemical and Biomolecular Engineering, Rice University, Houston, Texas 77005, United States;* orcid.org/0000-0002-5889-5009

Paul Westerhoff − *Nanosystems Engineering Research Center for Nanotechnology-Enabled Water Treatment, Houston, Texas 77005, United States; School of Sustainable Engineering and Built Environment, Arizona State University, Tempe, Arizona 85287, United States;* orcid.org/0000-0002-9241-8759

Xianghua Wen − *School of Environment, Tsinghua University, Beijing 100084, China;* orcid.org/0000-0002-9792-8678

Complete contact information is available at: https://pubs.acs.org/10.1021/acs.estlett.0c00434

Author Contributions

○L.D. and B.W. contributed equally to this work.

Notes

The authors declare no competing financial interest.

■ ACKNOWLEDGMENTS

This work was partially supported by the National Science Foundation Nanosystems Engineering Research Center for Nanotechnology-Enabled Water Treatment (EEC-1449500). L.D., B.W., and S.G. acknowledge support from the China Scholarship Council. The authors thank Prof. A. Martí and A. McWilliams for use of UV-DRS measurements, Mr. A. Nienhauser for assistance with chemical actinometry experiments, and Prof. J. Lou and T. Zhai for use of ball milling equipment.

■ REFERENCES

(1) Lin, H.; Wang, Y.; Niu, J.; Yue, Z.; Huang, Q. Efficient Sorption and Removal of Perfluoroalkyl Acids (PFAAs) from Aqueous Solution by Metal Hydroxides Generated in Situ by Electrocoagulation. *Environ. Sci. Technol.* **2015**, *49*, 10562−10569.

(2) Beesoon, S.; Martin, J. W. Isomer-Specific Binding Affinity of Perfluorooctanesulfonate (PFOS) and Perfluorooctanoate (PFOA) to Serum Proteins. *Environ. Sci. Technol.* **2015**, *49*, 5722−5731.

(3) Liu, Y.; Chen, S.; Quan, X.; Yu, H.; Zhao, H.; Zhang, Y. Efficient Mineralization of Perfluorooctanoate by Electro-Fenton with H2O2 Electro-generated on Hierarchically Porous Carbon. *Environ. Sci. Technol.* **2015**, *49*, 13528−13533.

(4) Huang, D.; Yin, L.; Niu, J. Photoinduced Hydrodefluorination Mechanisms of Perfluorooctanoic Acid by the SiC/Graphene Catalyst. *Environ. Sci. Technol.* **2016**, *50*, 5857−5863.

(5) Washington, J. W.; Jenkins, T. M. Abiotic Hydrolysis of Fluorotelomer-Based Polymers as a Source of Perfluorocarboxylates at the Global Scale. *Environ. Sci. Technol.* **2015**, *49*, 14129−14135.

(6) Washington, J. W.; Jenkins, T. M.; Rankin, K.; Naile, J. E. Decades-scale degradation of commercial, side-chain, fluorotelomer-based polymers in soils and water. *Environ. Sci. Technol.* **2015**, *49*, 915−923.

(7) Merino, N.; Qu, Y.; Deeb, R. A.; Hawley, E. L.; Hoffmann, M. R.; Mahendra, S. Degradation and Removal Methods for Perfluoroalkyl and Polyfluoroalkyl Substances in Water. *Environ. Eng. Sci.* **2016**, *33*, 615−649.

(8) Liu, Y.; Fan, X.; Quan, X.; Fan, Y.; Chen, S.; Zhao, X. Enhanced Perfluorooctanoic Acid Degradation by Electrochemical Activation of Sulfate Solution on B/N Codoped Diamond. *Environ. Sci. Technol.* **2019**, *53*, 5195−5201.

(9) Ochiai, T.; Iizuka, Y.; Nakata, K.; Murakami, T.; Tryk, D. A.; Koide, Y.; Morito, Y.; Fujishima, A. Efficient Decomposition of Perfluorocarboxylic Acids in Aqueous Suspensions of a TiO2Photocatalyst with Medium-Pressure Ultraviolet Lamp Irradiation under Atmospheric Pressure. *Ind. Eng. Chem. Res.* **2011**, *50*, 10943−10947.

(10) Giri, R. R.; Ozaki, H.; Okada, T.; Taniguchi, S.; Takanami, R. Factors influencing UV photodecomposition of perfluorooctanoic acid in water. *Chem. Eng. J.* **2012**, *180*, 197−203.

(11) Lee, Y. C.; Lo, S. L.; Chiueh, P. T.; Chang, D. G. Efficient decomposition of perfluorocarboxylic acids in aqueous solution using microwave-induced persulfate. *Water Res.* **2009**, *43*, 2811−6.

(12) Bentel, M. J.; Yu, Y.; Xu, L.; Li, Z.; Wong, B. M.; Men, Y.; Liu, J. Defluorination of Per- and Polyfluoroalkyl Substances (PFASs) with Hydrated Electrons: Structural Dependence and Implications to PFAS Remediation and Management. *Environ. Sci. Technol.* **2019**, *53*, 3718−3728.

(13) Zhang, C.; Qu, Y.; Zhao, X.; Zhou, Q. Photoinduced Reductive Decomposition of Perfluorooctanoic Acid in Water: Effect of Temperature and Ionic Strength. *Clean: Soil, Air, Water* **2015**, *43*, 223−228.

(14) Liang, X.; Cheng, J.; Yang, C.; Yang, S. Factors influencing aqueous perfluorooctanoic acid (PFOA) photodecomposition by VUV irradiation in the presence of ferric ions. *Chem. Eng. J.* **2016**, *298*, 291−299.

(15) Qian, Y.; Guo, X.; Zhang, Y.; Peng, Y.; Sun, P.; Huang, C.-H.; Niu, J.; Zhou, X.; Crittenden, J. C. Perfluorooctanoic Acid Degradation Using UV−Persulfate Process: Modeling of the Degradation and Chlorate Formation. *Environ. Sci. Technol.* **2016**, *50*, 772−781.

(16) Bao, Y.; Deng, S.; Jiang, X.; Qu, Y.; He, Y.; Liu, L.; Chai, Q.; Mumtaz, M.; Huang, J.; Cagnetta, G.; Yu, G. Degradation of PFOA Substitute: GenX (HFPO-DA Ammonium Salt): Oxidation with UV/Persulfate or Reduction with UV/Sulfite? *Environ. Sci. Technol.* **2018**, *52*, 11728−11734.

(17) Stancl, H. O. N.; Hristovski, K.; Westerhoff, P. Hexavalent Chromium Removal Using UV-TiO2/Ceramic Membrane Reactor. *Environ. Eng. Sci.* **2015**, *32*, 676−683.

(18) Wang, Y.; Zhang, P. Photocatalytic decomposition of perfluorooctanoic acid (PFOA) by TiO2 in the presence of oxalic acid. *J. Hazard. Mater.* **2011**, *192*, 1869−1875.
(19) Sansotera, M.; Persico, F.; Pirola, C.; Navarrini, W.; Di Michele, A.; Bianchi, C. L. Decomposition of perfluorooctanoic acid photocatalyzed by titanium dioxide: Chemical modification of the catalyst surface induced by fluoride ions. *Appl. Catal., B* **2014**, *148*−*149*, 29−35.
(20) Chen, Y. C.; Lo, S. L.; Kuo, J. Effects of titanate nanotubes synthesized by a microwave hydrothermal method on photocatalytic decomposition of perfluorooctanoic acid. *Water Res.* **2011**, *45*, 4131−4140.
(21) Zhao, B.; Zhang, P. Photocatalytic decomposition of perfluorooctanoic acid with β-Ga2O3 wide bandgap photocatalyst. *Catal. Commun.* **2009**, *10*, 1184−1187.
(22) Li, X.; Zhang, P.; Jin, L.; Shao, T.; Li, Z.; Cao, J. Efficient photocatalytic decomposition of perfluorooctanoic acid by indium oxide and its mechanism. *Environ. Sci. Technol.* **2012**, *46*, 5528−5534.
(23) Sahu, S. P.; Qanbarzadeh, M.; Ateia, M.; Torkzadeh, H.; Maroli, A. S.; Cates, E. L. Rapid Degradation and Mineralization of Perfluorooctanoic Acid by a New Petitjeanite Bi3O(OH)(PO4)2 Microparticle Ultraviolet Photocatalyst. *Environ. Sci. Technol. Lett.* **2018**, *5*, 533−538.
(24) Liu, Q.; Yu, Z. B.; Zhang, R. H.; Li, M. J.; Chen, Y.; Wang, L.; Kuang, Y.; Zhang, B.; Zhu, Y. H. Photocatalytic Degradation of Perfluorooctanoic Acid by Pd-TiO2 Photocatalyst. *Huan Jing Ke Xue* **2015**, *36*, 2138−2146.
(25) Mitchell, S. M.; Ahmad, M.; Teel, A. L.; Watts, R. J. Degradation of Perfluorooctanoic Acid by Reactive Species Generated through Catalyzed H2O2 Propagation Reactions. *Environ. Sci. Technol. Lett.* **2014**, *1*, 117−121.
(26) Li, X.; Li, Z.; Yang, J. Proposed Photosynthesis Method for Producing Hydrogen from Dissociated Water Molecules Using Incident Near-Infrared Light. *Phys. Rev. Lett.* **2014**, *112*, 018301.
(27) Shirodkar, S. N.; Waghmare, U. V.; Fisher, T. S.; Grau-Crespo, R. Engineering the electronic bandgaps and band edge positions in carbon-substituted 2D boron nitride: a first-principles investigation. *Phys. Chem. Chem. Phys.* **2015**, *17*, 13547−13552.
(28) Singh, B.; Kaur, G.; Singh, P.; Singh, K.; Sharma, J.; Kumar, M.; Bala, R.; Meena, R.; Sharma, S. K.; Kumar, A. Nanostructured BN−TiO2 composite with ultra-high photocatalytic activity. *New J. Chem.* **2017**, *41*, 11640−11646.
(29) Fu, X.; Hu, Y.; Yang, Y.; Liu, W.; Chen, S. Ball milled h-BN: An efficient holes transfer promoter to enhance the photocatalytic performance of TiO2. *J. Hazard. Mater.* **2013**, *244*−*245*, 102−110.
(30) Loeb, S. K.; Alvarez, P. J. J.; Brame, J. A.; Cates, E. L.; Choi, W.; Crittenden, J.; Dionysiou, D. D.; Li, Q.; Li-Puma, G.; Quan, X.; Sedlak, D. L.; David Waite, T.; Westerhoff, P.; Kim, J.-H. The Technology Horizon for Photocatalytic Water Treatment: Sunrise or Sunset? *Environ. Sci. Technol.* **2019**, *53*, 2937−2947.
(31) Liu, D.; Xiu, Z.; Liu, F.; Wu, G.; Adamson, D.; Newell, C.; Vikesland, P.; Tsai, A.-L.; Alvarez, P. J. Perfluorooctanoic acid degradation in the presence of Fe (III) under natural sunlight. *J. Hazard. Mater.* **2013**, *262*, 456−463.
(32) Qureshi, M.; Takanabe, K. Insights on measuring and reporting heterogeneous photocatalysis: efficiency definitions and setup examples. *Chem. Mater.* **2017**, *29*, 158−167.
(33) Kisch, H.; Bahnemann, D. Best Practice in Photocatalysis: Comparing Rates or Apparent Quantum Yields? *J. Phys. Chem. Lett.* **2015**, *6*, 1907−1910.
(34) Goto, H.; Hanada, Y.; Ohno, T.; Matsumura, M. Quantitative analysis of superoxide ion and hydrogen peroxide produced from molecular oxygen on photoirradiated TiO2 particles. *J. Catal.* **2004**, *225*, 223−229.
(35) Huang, D.; de Vera, G. A.; Chu, C.; Zhu, Q.; Stavitski, E.; Mao, J.; Xin, H.; Spies, J. A.; Schmuttenmaer, C. A.; Niu, J.; Haller, G. L.; Kim, J.-H. Single-Atom Pt Catalyst for Effective C−F Bond Activation via Hydrodefluorination. *ACS Catal.* **2018**, *8*, 9353−9358.
(36) Radhakrishnan, S.; Das, D.; Samanta, A.; de los Reyes, C. A.; Deng, L.; Alemany, L. B.; Weldeghiorghis, T. K.; Khabashesku, V. N.; Kochat, V.; Jin, Z.; et al. Fluorinated h-BN as a magnetic semiconductor. *Sci. Adv.* **2017**, *3*, No. e1700842.
(37) Li, L. H.; Chen, Y. Atomically thin boron nitride: unique properties and applications. *Adv. Funct. Mater.* **2016**, *26*, 2594−2608.
(38) Ding, Y.; Torres-Davila, F.; Khater, A.; Nash, D.; Blair, R.; Tetard, L. Defect engineering in Boron Nitride for catalysis. *MRS Commun.* **2018**, *8*, 1236−1243.
(39) Hogue, C. What's GenX still doing in the water downstream of a Chemours plant? *Chem. Eng. News* **2018**, *96*.

https://dx.doi.org/10.1021/acs.estlett.0c00434
Environ. Sci. Technol. Lett. XXXX, XXX, XXX−XXX